Environ. Eng. Res. 2021; 26(2): 200043
https://doi.org/10.4491/eer.2020.043

pISSN 1226-1025
eISSN 2005-968X

Research

# Inhibiting oxidation and enhancing absorption characteristics of sodium sulfite for $SO_2$ removal from the non-ferrous smelting flue gas

**Yongpeng Ma[1†], Dongli Yuan[1], Xiaojing Zhang[1], Zan Qu[2], Wenjun Huang[2]**

[1]*Henan Collaborative Innovation Center of Environmental Pollution Control and Ecological Restoration, School of Material and Chemical Engineering, Zhengzhou University of Light Industry, No. 136, Science Avenue, Zhengzhou 450001, China*
[2]*School of Environmental Science and Engineering, Shanghai Jiao Tong University, Shanghai 200240, China*

**ABSTRACT**

In this work, we investigated the absorption characteristics of $SO_2$ and the effect of inhibitors on the desulfurization performances of $Na_2SO_3$. The results showed that the $NO_2$ had a competitive effect with $SO_2$ on $SO_3^{2-}$ which resulted in a significant decrease in the absorption capacity of $SO_2$. $O_2$ in the flue gas could decrease the absorption capacity of $SO_2$ due to the oxidation of $Na_2SO_3$. Besides, $Na_2S_2O_3$ had more excellent inhibiting effect on the oxidation of $SO_3^{2-}$; the inhibition mechanism is understood on the basis of the free radical chain reaction, whereby $S_2O_3^{2-}$ combined with the sulfite free radical to form an inert substance, thus, quenching the reaction of free radical with the dissolved oxygen and invariably inhibiting the oxidation of $SO_3^{2-}$. Furthermore, the intrinsic and the apparent oxidation kinetics of $Na_2SO_3$ oxidation process with $Na_2S_2O_3$ were investigated to explain the relationships between consumption rates of $SO_3^{2-}$ and the absorption capacities of $SO_2$ under different components in flue gas and absorption solution.

**Keywords:** Absorption characteristic, Desulfurization, Inhibiting oxidation, Smelting flue gas, Sodium sulfite

## 1. Introduction

The northern area of China has witnessed incessant haze pollution in recent years. This predominant in cities with high industrial activities, and occurs mainly during the winter or spring season [1-2]. The major component of haze is the particulate matter (PM). $PM_{2.5}$ (particulate matter with diameters less than 2.5 $\mu$m) have more concentrations and it is more harmful to human health, this is mainly attributed to its small size which is an influential factor to visibility since mass extinction efficiency of $PM_{2.5}$ is 7 times of larger particles. Moreover, the deterioration of air quality and haze episodes illustrates that $PM_{2.5}$ plays a dominant role in the formation of smog [3-4]. The visible light absorption and scattering were affected by the gaseous pollutants in the air and the chemical compositions of $PM_{2.5}$ [5]. Sulfur dioxide ($SO_2$) is the primary haze pollutant and contributes significantly to the nucleation, toxicity, and complexity of $PM_{2.5}$ [6-8]; hence controlling its emission is of paramount importance. Furthermore, it has been reported that sulfate, nitrate, and ammonium (SNA) which are referred to as secondary inorganic aerosols contribute to approximately 27 % of the $PM_{2.5}$.

To ensure that the $SO_2$ and $NO_X$ emissions from flue gases are reduced to the barest minimum, the desulfurization and denitrification technologies in coal-fired power plants and the industrial boilers have been developed for years in compliance with the stringent emission standard [9-13]. However, the $SO_2$ emission from the non-ferrous metal smelting flue gas has received little attention in the past, hence, the control of $SO_2$ emission has not been optimized [14].

In a typical smelting process, a high concentration of $SO_2$ (> 4%) can be directly converted to sulfuric acid by double-conversion double-absorption (DCDA) process downstream of the dust removal devices and dynamic wave scrubbing units [15]. While for the $SO_2$ concentration in the range of 2 – 4% in flue gas, single-conversion single-absorption (SCSA) process is employed to produce



**Received** January 28, 2020 **Accepted** April 03, 2020

† Corresponding author
Email: mayongpeng1984@163.com
Tel: +86-150-0383-5272 Fax: +86-371-86609680
ORCID: 0000-0003-2983-9435

sulfuric acid and the $SO_2$ in the exhaust gas can be absorbed by sodium hydroxide. However, when $SO_2$ in flue gas is lower than 2%, it cannot be used for the conversion of sulfuric acid due to its low concentration. Wet scrubbing technology using sodium hydroxide is adopted for desulfurization in these smelting factories. The concentration of $SO_2$ was still too high to be controlled, unlike the concentration of gases from coal-fired flue gas.

The use of sodium hydroxide, sodium citrate process, organic amine process, ionic liquid process, magnesium process, and sodium sulfite process for the removal of $SO_2$ from characteristics flue gas have been investigated and implemented, but these processes are not economical. Moreover, they lead to heavy metal pollution and hazardous waste generation [16-19]. Sodium sulfite process (Wellman-Lord Process) is one of the most efficient technique for the desulfurization and recovery of $SO_2$, due to its relatively high efficiency and low energy consumption [20]. However, sodium sulfite process is offset by the reduction in the desulfurization efficiency, which is the consequence of $Na_2SO_3$ oxidation in the absorption solution. The following equations show the main absorption and oxidation processes of $Na_2SO_3$ [21]:

$$Na_2SO_3 + SO_2 + H_2O = 2NaHSO_3 \quad (1)$$

$$2Na_2SO_3 + O_2 = 2Na_2SO_4 \quad (2)$$

$$6NaHSO_3 = 2Na_2SO_4 + Na_2S_2O_3 + 3H_2O + SO_2 \quad (3)$$

It was reported that the oxidation of sulfite was a free radical reaction. Sipos et al. [22] selected phenol as the appropriate inhibitor. However, phenol was not acceptable for real applications because it is also an environmental pollutant. Cui *et al.* reported that the hydroxyl functional group in TP (Tea Polyphenols) makes the ring become active and reductive, hence TP can be effectively used as an additive. The chain reaction of sulfite oxidation was broken and inhibited [23]. Wang et al. [24] studied the effect of ethanol on the oxidation of $Na_2SO_3$ and reported that ethanol inhibited the oxidation of sulfite. The mechanism of inhibition of sodium sulfite oxidation and the inhibition kinetics of sulfite oxidation by ethanol was proposed. However, previous studies primarily focused on selecting inhibitors of sulfite oxidation and investigating the inhibition mechanism, but they are not applicable in non-ferrous smelting industries. The selection and inhibition mechanism of complex flue gas with high concentrations of $SO_2$, $NO_X$, and $O_2$ is not fully understood, hence, it requires further studies. Besides, the relationships between desulfurization performances and the sodium sulfite added inhibitors are still ambiguous, and the effects of complex components in smelting flue gas on the inhibitors are not clear.

In this study, we investigated the absorption characteristics of $SO_2$ along with the intrinsic and apparent oxidation kinetics of $SO_3^{2-}$ in the cyclic sodium sulfite absorption system. The related kinetic parameters and mechanism of inhibition oxidation were obtained by investigating the relationship between the consumption rate of $SO_3^{2-}$ and the absorption time of $SO_2$ under different components in flue gas and absorption solution with $Na_2S_2O_3$ inhibitor. The results will provide a theoretical basis for $SO_2$ emission control and resource recovery from non-ferrous metal smelting flue gas.

## 2. Experimental Apparatus and Methods

### 2.1. Experimental Apparatus

A schematic diagram of the experimental apparatus was shown in Fig. S1 (as shown in supplementary material), and it is made up of the simulated flue gas distribution system, the absorption reaction system, the online monitoring system, and the exhaust gas treatment system. The simulated flue gas was supplied by the cylinders at a flow rate of 1.0 L/min. The components in flue gas were 5000 mg/m$^3$ $SO_2$, 600 mg/m$^3$ $NO_2$, 0 - 8 % $O_2$ and $N_2$ of the carrier gas. All the gases were controlled by mass flow meters. The $SO_2$ absorption experiments were carried out in a three-port bubbling reactor with 50 mL of 2 – 4% $Na_2SO_3$ solution. The temperatures of flue gas and absorption solution were 323K and 293 K, respectively. The flue gas from the outlet was continuously absorbed by 5% NaOH and 5% $KMnO_4$ solution so that the exhaust gas was purified and discharged.

The concentration of $SO_2$ and $NO_X$ in the inlet and outlet of the reactor was monitored by a flue gas analyzer (Testo-350, Germany).

### 2.2. Materials

The main chemicals and consumables used in this study are stated below: sodium sulfite (99%), sodium thiosulfate (99%), sodium sulfate (98%), sodium nitrite (99%), anhydrous ethanol and triethanolamine from Sigma-Aldrich Co, Ltd. The $SO_2$ (5%), $O_2$ (99.9%), $NO_2$ (1%) and $N_2$ (99.9%) were obtained from Henan Yuanzheng Gas Co., Ltd and stored in cylinders.

### 2.3. Methods

The removal efficiencies of $SO_2$ were calculated by the following Eq. (4):

$$\eta_{SO_2} = \frac{C_{SO_{2(i)}} - C_{SO_{2(O)}}}{C_{SO_{2(i)}}} \times 100\% \quad (4)$$

Where $\eta_{SO2}$ is the removal efficiency of $SO_2$, and $C_{SO2(i)}$ and $C_{SO2(O)}$ are the sulfur dioxide inlet concentration and outlet concentration, respectively.

The absorption capacities of $SO_2$ in $Na_2SO_3$ solution were calculated by integrating the absorption curve as shown in Eq. (5).

$$\tau = \frac{1}{V}\int_{t_2}^{t_1}(C_{(i)} - C_{(o)}) \times f \times dt \quad (5)$$

where $\tau$ is the absorption capacity of $SO_2$, and $C_{(i)}$ and $C_{(o)}$ are the concentrations of the $SO_2$ inlet and outlet, respectively. V is the volume of $Na_2SO_3$ solution. $t_1$ and $t_2$ are the starting and ending time of absorption, respectively. f is the flue gas flow.

The consumption of $Na_2SO_3$ was deduced from the Eq. (1) so that the utilization ratio of $Na_2SO_3$ was obtained by the following Eq. (6):

$$\eta_{1Na_2SO_3} = \frac{m_{Na_2SO_{3(c)}}}{m_{Na_2SO_{3(t)}}} \times 100\% \quad (6)$$

where $\eta_{1Na2SO3}$ is the utilization ratio of sodium sulfite, and $m_{Na2SO3(t)}$

and $m_{Na2SO3(c)}$ are the total amount of sodium sulfite and the amount of sodium sulfite consumed by absorbing $SO_2$, respectively.

The intrinsic oxidation kinetics parameters and inhibition mechanism of $Na_2SO_3$ were obtained by the following methods. $Na_2SO_3$ reacted with dissolved oxygen according to the Eq. (7). The dissolved oxygen meter records the concentration of dissolved oxygen in solution. Compared with the initial concentration of $SO_3^{2-}$ ($C_2$) and dissolved oxygen ($C_3$), the initial concentration of the inhibitor ($C_1$) is negligible. At any time, the consumed dissolved oxygen is marked to $C_{3i}$, and the concentration of oxidized $SO_3^{2-}$ is 2 ($C_{3i}$), and then plotted as 2 ($C_{3i}$)-t. The slope of the obtained straight line is the intrinsic oxidation rate of $SO_3^{2-}$.

$$SO_3^{2-} + 1/2O_2 \longrightarrow SO_4^{2-} \quad (7)$$

When the temperature is constant, the reaction rate of $SO_3^{2-}$ at different initial $Na_2S_2O_3$ concentration ($C_i$) is determined, and then plotting with Ln(r)- Ln($c_i$), the slope of the obtained straight line is the reaction order of the inhibitor. Similarly, by measuring the reaction rate of $SO_3^{2-}$ at different initial $Na_2SO_3$ concentrations ($C_j$), and then plotting it with Ln (r) -Ln ($C_j$), the slope of the obtained straight line is the reaction order of $SO_3^{2-}$.

The apparent oxidation kinetic parameters and inhibition mechanism of $Na_2SO_3$ could be obtained by the following methods. The liquid samples taken from the experiment were quantitatively analyzed by Dionex Aquion analytical multi-function ion chromatography (Dionex Aquion, Thermo Scientific, America). The generated $SO_4^{2-}$ concentration ($C_{4i}$) at different absorption times was measured, and then plotted as $C_{4i}$-t. The slope of the obtained straight line was the $SO_4^{2-}$ generation rate. Similarly, by measuring the $SO_4^{2-}$ generation rate at different initial $Na_2S_2O_3$ concentrations ($C_k$), and then plotting it with Ln (r) -Ln ($C_k$), the slope of the obtained straight line is the reaction order of the inhibitor.

## 3. Results and Discussion

### 3.1. Effects of Flue Gas Components on Desulfurization Performance

The effects of the primary gas components on desulfurization performance were investigated and the results are shown in Fig. 1. The total flow rate of the simulated flue gas was 1.0 L/min. The initial $SO_2$ concentration was 5,000 mg/m$^3$, and the $Na_2SO_3$ mass concentration was 2%. The results showed that $O_2$ and $NO_2$ in flue gas had a significant effect on the effective desulfurization time, but had a negligible effect on the maximum desulfurization efficiency. Curves of a, b, and d in Fig. 1 revealed that the absorption capacity of $SO_2$ decreased with the presence of $O_2$ in the flue gas. The higher the $O_2$ concentration, the smaller the absorption capacity of $SO_2$. This may be attributed to the consumption of $SO_3^{2-}$ by $O_2$, as shown in the Eq. (2). When the oxygen concentration increased from 0 to 6%, the absorption capacities of $SO_2$ decreased from 9.96 to 8.69g/L, respectively. Accordingly, the increase in the concentration of $SO_4^{2-}$ from 0 to 5.86g/L detected in the absorption solution indicated that part of $SO_3^{2-}$ was directly oxidized to $SO_4^{2-}$, thereby reducing its participation in the $SO_2$ absorption reaction.

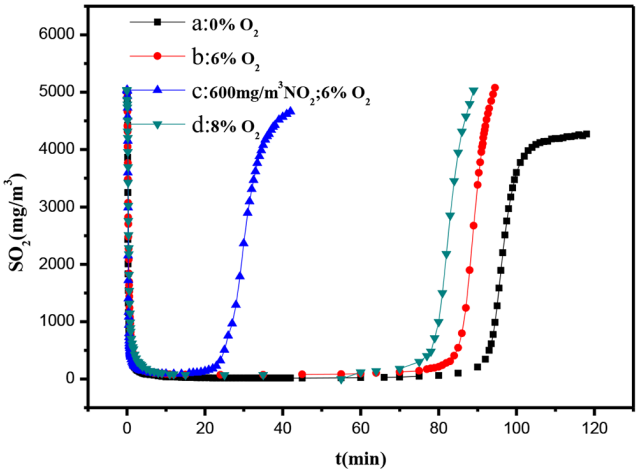


**Fig. 1.** Effects of flue gas components on desulfurization performances.

Denitration in a non-ferrous metal smelting flue gas usually involves the oxidation of NO to $NO_2$ by ozone and the absorption by aqueous solution. As can be seen from the curves of b and c in Fig. 1, when $NO_2$ was introduced into the flue gas, the absorption capacities of $SO_2$ decreased from 8.69 to 3.04g/L, which indicated that $NO_2$ in flue gas is unfavorable for the absorption of $SO_2$. Irrespective of its excellent solubility in water, $NO_2$ still have a poor absorption effect in aqueous solution than in $Na_2SO_3$ solution from Fig. S2. The absorption of $NO_2$ by $Na_2SO_3$ solution certified that $NO_2$ and $SO_2$ had a competitive effect on $SO_3^{2-}$. The consumption of $SO_3^{2-}$ by $NO_2$ as shown in the Eq. (8)-(11) is the main reason for the decrease in the absorption capacity of $SO_2$. After the absorption of pure $NO_2$ by $Na_2SO_3$, the $SO_3^{2-}$ in the absorption solution was converted to $SO_4^{2-}$, this observation validates the role of Eq. (8)-(11) in the absorption system.

The absorption curves of $SO_2$ with the presence of $NO_2$ were shown in Fig. S3. Compared with curve b in Fig. 1, the absorption capacity of $SO_2$ decreased from 8.69 g/L to 3.04 g/L. Compared with the absorption of $NO_2$ by 2% $Na_2SO_3$ in Fig. S2, the absorption capacity of $NO_2$ decreased from 0.33 g/L to 0.21 g/L, which proved that $NO_2$ and $SO_2$ had competitive effects on $SO_3^{2-}$.In addition, $NO_2$ is absorbed to form $NO_2^-$, which can react with $SO_3^{2-}$ to form the intermediate sulfur nitrogen compound, which can be stable at a high S/N ratio and low pH [25, 26]. The reaction equation involved is shown as Eq. (8)-(11):

$$SO_3^{2-} + 2NO_2 + H_2O \rightarrow 2NO_2^- + SO_4^{2-} + 2H^+ \quad (8)$$

$$HSO_3^- + 2NO_2 + H_2O \rightarrow 2NO_2^- + SO_4^{2-} + 3H^+ \quad (9)$$

$$SO_3^{2-} + 2NO_2^- + 4H^+ \rightarrow 2NO + 2H_2O + H_2SO_4 \quad (10)$$

$$NO_2^- + H^+ + HSO_3^- \rightarrow ONSO_3^- + H_2 \quad (11)$$

### 3.2. Selection of Oxidation Inhibitor for S(IV)

To inhibit the oxidation of $Na_2SO_3$, the effects of different inhibitors on the desulfurization performances of $Na_2SO_3$ were investigated.

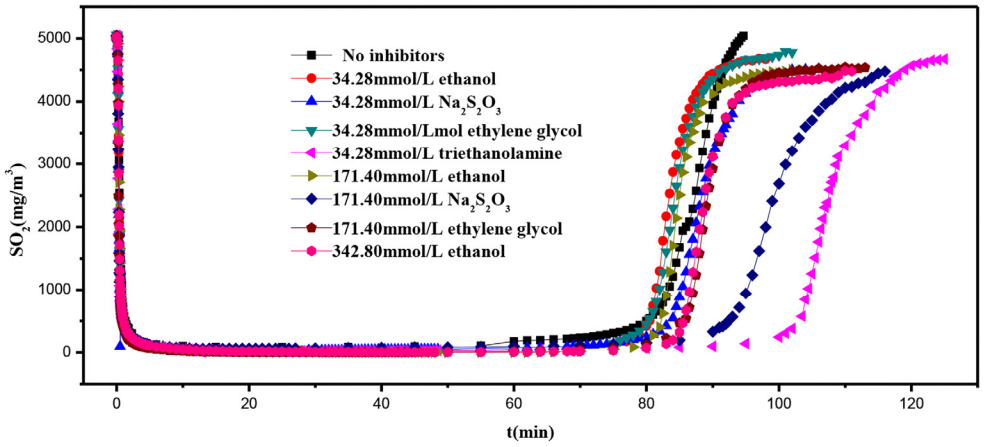


**Fig. 2.** Effect of different additives on desulfurization performances.

The results are shown in Fig. 2. When 34.28 mmol/L of ethanol was added into the absorption solution, the absorption capacity of $SO_2$ increased from 8.47 to 8.49 g/L, and the utilization rate of $Na_2SO_3$ increased from 83.37% to 83.57%, indicating that ethanol had a slight inhibiting effect on the oxidation of $SO_3^{2-}$. However, increasing the concentration of ethanol in the absorption solution did not promote the inhibiting effect of ethanol on the oxidation of $SO_3^{2-}$, this observation is attributed to the expulsion of excessive ethanol from the absorption system by the simulated flue gas. Moreover, this assertion is also validated by the presence of ethanol detected in the tail gas.

When ethylene glycol was added as an inhibitor to the absorption solution, the oxidation of $SO_3^{2-}$ was also inhibited. The ethylene glycol will act as the $\bullet SO_3^-$ radical-trapping material and break the chain by reacting with the $\bullet SO_3^-$ radical. Finally, ethylene glycol may generate aldehyde or carboxylate as a result of induced oxidation of ethylene glycol. Increasing the concentration of ethylene glycol led to an insignificant improvement in its inhibiting effect. It can be seen from Fig. 2 that when $Na_2S_2O_3$ was used as an inhibitor, the absorption capacity of $SO_2$ increased obviously.

Also, the inhibiting effect of triethanolamine on oxidation of $SO_3^{2-}$ was investigated. As seen from Fig. 2, the absorption capacities of $SO_2$ increased to 28.45% after the addition of 34.28 mmol/L of triethanolamine into the absorption solution, which primarily indicated that triethanolamine can promote $SO_2$ absorption in this system. However, the triethanolamine solution presents alkaline and produces ammonium ions, which may be one of the reasons for promoting the absorption capacity of $SO_2$. Therefore, further exploration was preceded and the results were shown in Fig. 3. In comparison with 2% $Na_2SO_3$, the pure 0.2% triethanolamine absorbed more $SO_2$. Therefore, the addition of triethanolamine mainly promotes the absorption capacity of $SO_2$ Eq. (12), and to some extent, inhibits the oxidation of $SO_3^{2-}$.

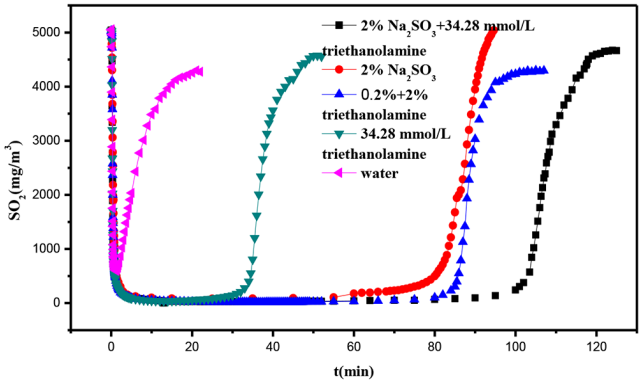


**Fig. 3.** Effect of different triethanolamine content on desulfurization performances.

$$N(CH_2CH_2OH)_3 + SO_2 = \left(\begin{matrix}(OCH_2CH_2)_2\\HOCH_2CH_2\end{matrix}\right)N=S\begin{matrix}O\\O\end{matrix}\Big)_4^{2-} + 2H^+ \quad (12)$$

By comparison, the inhibiting effect of $Na_2S_2O_3$ on oxidation of $SO_3^{2-}$ was more excellent and matched with the $Na_2SO_3$ desulfurization system. Then, the effects of $Na_2S_2O_3$ as an inhibitor on the desulfurization of the $Na_2SO_3$ system were investigated.

### 3.3. Effects of $Na_2S_2O_3$ Inhibitor on Desulfurization Performance

Increasing $Na_2SO_3$ concentration can improve desulfurization efficiency and increase the absorption capacity of $SO_2$. However, it also increased the oxidation rate of $SO_3^{2-}$, resulting in a lower utilization rate of $Na_2SO_3$. The effects of $Na_2SO_3$ concentration on desulfurization were investigated at a constant $Na_2S_2O_3$ concentration. From Fig. 4(a), in the absence of $Na_2SO_3$, the absorption capacities of $SO_2$ by 2%, 3% and 4% $Na_2SO_3$ was 8.83g/L, 11.77 g/L, 15.06 g/L, and the utilization rate of $Na_2SO_3$ was 86.88%, 77.22%, and 74.11%, respectively. When $Na_2S_2O_3$ was added into the absorption solution as an inhibitor, the absorption capacities of $SO_2$ by 2%, 3% and 4% $Na_2SO_3$ were increased to 19.48%, 31.52%, and 33.07%, respectively.

In order to clarify the dosage relationship between $Na_2S_2O_3$ and the oxidation of $Na_2SO_3$, the inhibiting effects of $Na_2S_2O_3$ concentration were investigated at constant $Na_2SO_3$ concentration. As seen from Fig. 5, pure $Na_2S_2O_3$ solution had poor desulfurization efficiency, but the absorption capacity of $SO_2$ was enhanced significantly after adding $Na_2S_2O_3$ as an inhibitor. The absorption capacity of $SO_2$ increased progressively with the increase in $Na_2S_2O_3$

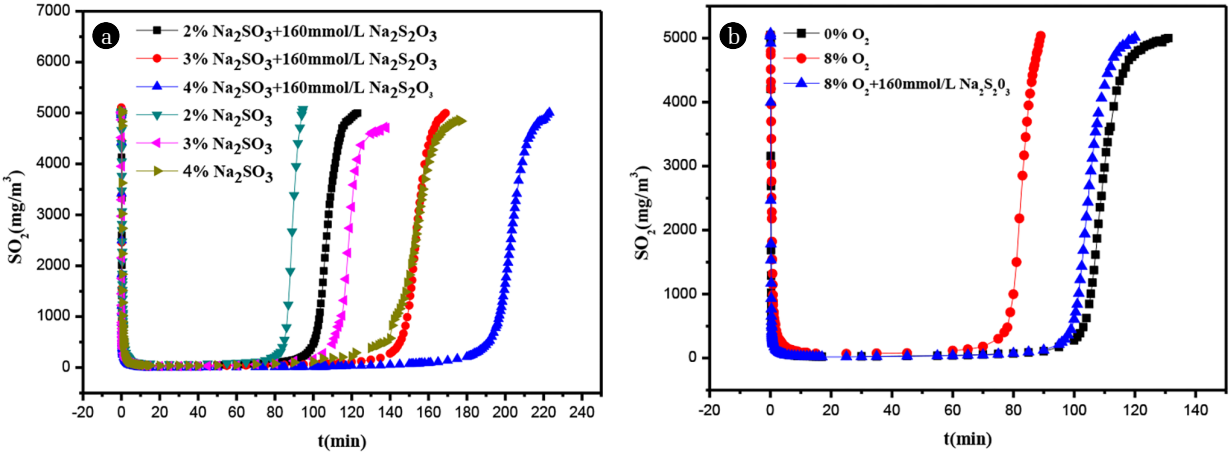


**Fig. 4.** (a) Effect of $Na_2SO_3$ Concentration on Desulfurization Performance, (b) Effect of oxygen content on desulfurization performance of $Na_2SO_3$.

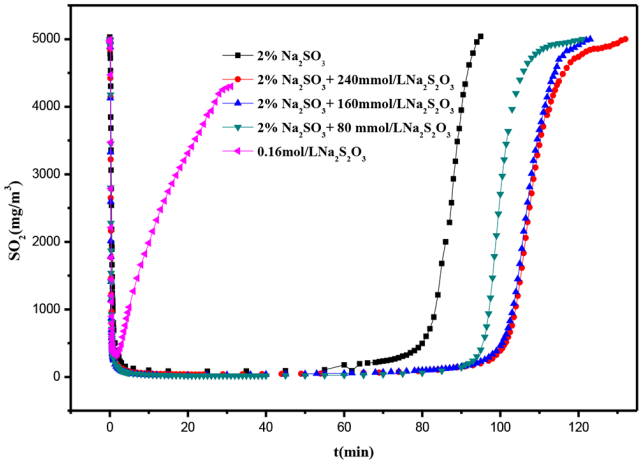


**Fig. 5.** Effect of $Na_2S_2O_3$ concentration on desulfurization performance.

concentration and attained a maximum level when the concentration of $Na_2S_2O_3$ is 240 mmol/L. Therefore, the concentration of $Na_2S_2O_3$ should be matched with the concentration of $Na_2SO_3$ to optimize the dosage of inhibitors.

The oxidation of $Na_2SO_3$ was prompted by the oxygen from the flue gas which dissolved into the absorption solution and reacted with $SO_3^{2-}$ to produce stable $SO_4^{2-}$, so the concentration of oxygen in the flue gas was also one of the main factors affecting the $SO_2$ removal. As shown in Fig. 4(b), the increase of oxygen concentration without inhibitor led to the increase in the oxidation rate of $SO_3^{2-}$ and the decrease in the absorption capacity of $SO_2$. When $Na_2S_2O_3$ was added as an inhibitor, the increase in oxygen concentration had little influence on the oxidation rate of $SO_3^{2-}$ and absorption capacity of $SO_2$.

The inhibition mechanism of $Na_2S_2O_3$ on the oxidation of $Na_2SO_3$ may be summarized as follows: the oxidation reaction of $SO_3^{2-}$ is a free radical chain reaction and the inhibitor mainly inhibits the oxidation of sulfite by preventing the chain reaction. The $S_2O_3^{2-}$ combines with the sulfite free radical to form an inert substance that prevents the sulfite free radical from further reacting with the dissolved oxygen. The reaction mechanisms are shown in Eqs. (13)-(16) [27]:

$$\cdot SO_3^- + S_2O_3^{2-} \rightarrow \cdot S_2O_3^- + SO_3^{2-} \quad (13)$$

$$\cdot SO_3^- + \cdot S_2O_3 \rightarrow \text{polythionates} \quad (14)$$

$$\cdot S_2O_3^- + \cdot S_2O_3^- \rightarrow \text{polythionates} \quad (15)$$

$$\text{polythionates} + H_2O \rightarrow S_2O_3^{2-} + SO_3^{2-} + 2H^+ \quad (16)$$

### 3.4. The Kinetics of $SO_3^{2-}$ Oxidation and Its Inhibition

The intrinsic oxidation kinetics and apparent oxidation kinetics of sulfite were studied to properly elucidate the oxidation mechanism of sulfite. The intrinsic oxidation kinetics are shown in Fig. 6 and Fig. 7. It can be seen from Fig. 6, when the concentration of $Na_2S_2O_3$ was 0.10, 0.15 and 0.2mmol/L, respectively. The initial concentration method was used to obtain the reaction rate of sulfite under different inhibitor concentrations. The sulfite concentration and reaction rate was dimensionless with respect to the initial values. Therefore, as shown in Fig. 6, the reaction order of $Na_2S_2O_3$ was -2.22. This indicates that $Na_2S_2O_3$ inhibits sulfite oxidation significantly, and the sulfite oxidation rate decreased significantly with the increase in $Na_2S_2O_3$concentration.

The reaction order of sodium sulfite under different initial $Na_2SO_3$ concentration was shown in Fig. 7. When 0.20 mmol/L of $Na_2S_2O_3$ was added, and the initial concentration of sodium sulfite was 4, 6, 8, 10 mmol/L, the sulfite concentration and reaction rate was dimensionless with respect to the initial values. Therefore, the reaction order of $Na_2SO_3$ as shown in Fig. 7 was 2.393, which indicates that the oxidation rate of sulfite increases with the increase in the initial concentration of $Na_2SO_3$.

The apparent oxidation kinetics mechanism was obtained by analyzing the composition of the desulfurization solution. Dionex Aquion analytical multi-function ion chromatography was used to quantitatively analyze the desulfurization solution with or without inhibitor. As can be seen from Fig. 8, the rate of sulfate formation was 53.08 mg/(L·min) in the absence of inhibitor. When 240mmol/L of inhibitor was added, the rate of sulfate formation was 7.28 mg/(L·min), which indicated that $Na_2S_2O_3$ inhibits sulfite oxidation, thereby reducing the rate of sulfate formation.

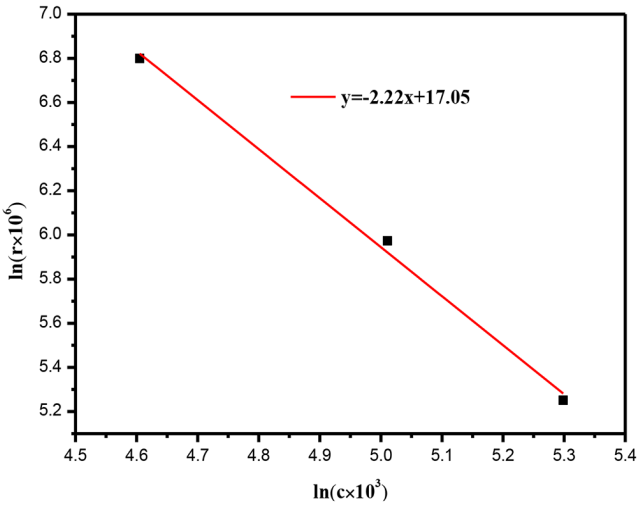


**Fig. 6.** Reaction order of $Na_2S_3O_3$.

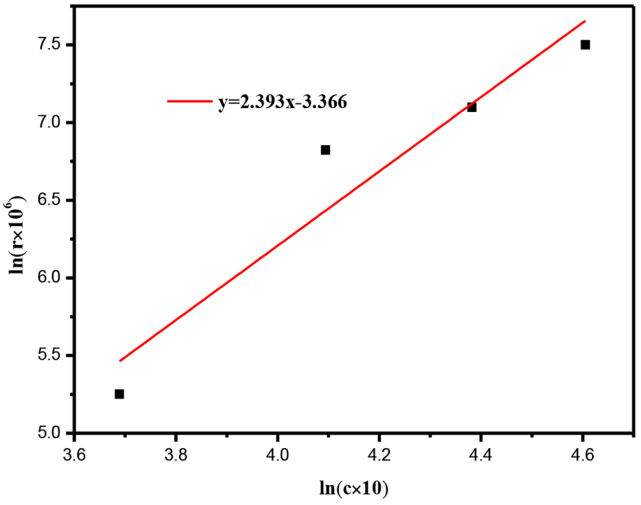


**Fig. 7.** Reaction order of sulfite.

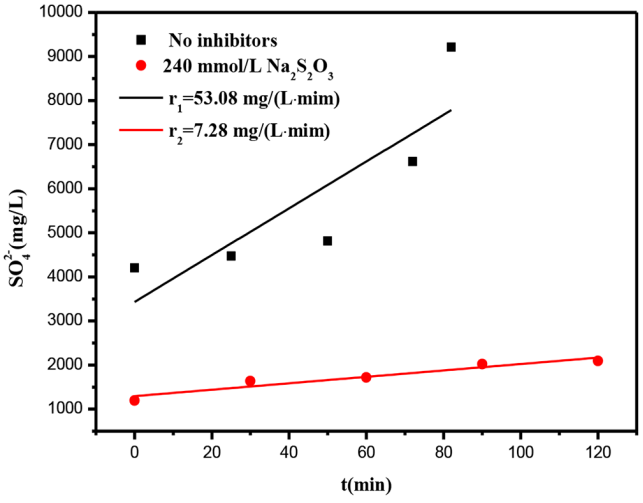


**Fig. 8.** Effect of $Na_2S_2O_3$ on sulfate formation rate.

The reaction order of sulfate at different initial $Na_2S_2O_3$ concentration was shown in Fig. S3. On the addition of 80, 160, and 240 mmol/L of $Na_2S_2O_3$, respectively, the sulfate content was determined by ion chromatography, from which the reaction rate was calculated. Since the sulfate concentration and the reaction rate are dimensionless with respect to the initial value. Therefore, the reaction order of $Na_2S_2O_3$ as shown in Fig. S3 was -1.35. This result revealed that $Na_2S_2O_3$ inhibits the rate of sulfate formation significantly, and the rate of sulfate formation decreases significantly with increasing concentration of $Na_2S_2O_3$.

## 4. Conclusions

In this study, a new cyclic sodium sulfite process was proposed to remove $SO_2$ from a non-ferrous metal smelting flue gas. The effects of different components of flue gas on desulfurization performance were investigated, and the results indicated that the $NO_2$ had a competitive effect with $SO_2$ on $SO_3^{2-}$ which led to a significant decrease in the absorption capacity of $SO_2$. The $O_2$ in the flue gas contributed to the decrease in the absorption capacity of $SO_2$ due to its oxidative effect on $Na_2SO_3$. By comparison, the inhibiting effect of $Na_2S_2O_3$ on the oxidation of $SO_3^{2-}$ was more excellent and matched with the $Na_2SO_3$ desulfurization system. The inhibition mechanism is understood on the basis of the free radical chain reaction, whereby $S_2O_3^{2-}$ combined with the sulfite free radical to form an inert substance, thus, quenching the reaction of free radical with the dissolved oxygen and invariably inhibiting the oxidation of $SO_3^{2-}$.

In addition, the intrinsic oxidation kinetics showed that the reaction order of $Na_2S_2O_3$ was -2.22, and the reaction order of $Na_2SO_3$ was 2.393. On the addition of 240 mmol/L of $Na_2S_2O_3$ in $Na_2SO_3$ solution, the apparent oxidation kinetics gave a sulfate formation rate of 7.28 mg/(L·min). However, in the absence of $Na_2S_2O_3$ in the $Na_2SO_3$ solution, the formation rate of sulfate was 53.08mg/(L·min). The reaction order of $Na_2S_2O_3$ was -1.35, which indicated that $Na_2S_2O_3$ has an excellent inhibiting effect on the oxidation of $SO_3^{2-}$and the desulfurization performances are improved significantly.

## Acknowledgment

This study was supported by the National Key R&D Program of China (No.2017YFC0210500), Key Scientific Research Project of Colleges in Henan Province-China (No.20A610011), the China Postdoctoral Science Foundation (No.2018M640393). This work was also funded by the Scientific and Technological Project of Henan Province-China (No. 202102310283).

## Author Contributions

YP.M. (Associate professor) contributed to the conception of the study. DL.Y. (Master student) conducted all the experiments and wrote the manuscript. XJ.Z. (Associate professor) contributed to

analysis and manuscript preparation. Z.Q. (Professor) performed the data measurement and analyses. WJ.H. (Associate professor) helped perform the analysis and writing examination.

## References


1. Miao XY, Zhan HL, Zhao K, et al. Terahertz-dependent $PM_{2.5}$ monitoring and grading in the atmosphere. *Sci. China Phys. Mech.* 2018;61:104211.
2. Jiang BF, Xie YL, Xia DH, Liu XJ. A potential source for $PM_{2.5}$: Analysis of fine particle generation mechanism in wet flue gas desulfurization system by modeling drying and breakage of slurry droplet. *Environ. Pollut.* 2019;246:249-256.
3. Cheng Z, Wang SX, Jiang JK, et al. Long-term trend of haze pollution and impact of particulate matter in the Yangtze River Delta, China. *Environ. Pollut.* 2013;182:101-110.
4. Zhu WF, Xie JK, Cheng Z, et al. Influence of chemical size distribution on optical properties for ambient submicron particles during severe haze events. *Atmos. Environ.* 2018;191: 162-171.
5. Yao S, Cheng SY, Li JB, Zhang HY, Jia J, Sun XW. Effect of wet flue gas desulfurization (WFGD) on fine particle ($PM_{2.5}$) emission from coal-fired boilers. *J. Environ. Sci.* 2019;77:32-42.
6. Ge XL, Li L, Chen YF, et al. Aerosol characteristics and sources in Yangzhou, China resolved by offline aerosol mass spectrometry and other techniques, *Environ. Pollut.* 2017;225:74-85.
7. Guo S, Hu M, Zamora ML, et al. Elucidating severe urban haze formation in China, *P. Natl. Acad. Sci. USA.* 2014;111: 17373-17378.
8. Li K, Chen L, White SJ, et al. Effect of nitrogen oxides (NO and $NO_2$) and toluene on $SO_2$ photo oxidation, nucleation and growth: A smog chamber study. *Atmos. Res.* 2017;192:38-47.
9. Ma SH, Wen ZG, Chen JN. Scenario Analysis of Sulfur Dioxide Emissions Reduction Potential in China's Iron and Steel Industry. *J. Ind. Ecol.* 2012;16:506-517.
10. Ding J, Zhong Q, Zhang SL, Song FJ, Bu YF, Simultaneous removal of $NO_X$ and $SO_2$ from coal-fired flue gas by catalytic oxidation-removal process with $H_2O_2$. *Chem. Eng. J.* 2014;243: 176-182.
11. Hao RL, Yang S, Yuan B, Zhao Y. Simultaneous desulfurization and denitrification through an integrative process utilizing $NaClO_2/Na_2S_2O_8$. *Fuel Process. Technol.* 2017;159:145-152.
12. Ma YP, Yuan DL, Mu BL, Gao L, Zhang XJ, Zhang HZ. Synthesis, properties and application of double salt $(NH_4)_2Mg(SO_4)_2{\cdot}6H_2O$ in wet magnesium-ammonia FGD process. *Fuel* 2018;219:12-16.
13. Yang BC, Ma SX, Cui RJ, Sun SJ, Wang J, Li SC. Simultaneous removal of $NO_X$ and $SO_2$ with $H_2O_2$ catalyzed by alkali/magnetism-modified fly ash: High efficiency, Low cost and Catalytic mechanism. *Chem. Eng. J.* 2019;359:233-243.
14. Gao L, Li Y, He J. Intensifying effects of zinc oxide wet flue gas desulfurization process with citric acid. *J. Environ. Chem. Eng.* 2019;7:102831.
15. Moeller W, Winkler K. The double contact process for sulfuric acid production. *J. Air Pollut. Contr. Assoc.* 1968;18:324-325.
16. Jiang XP, Liu YZ, Gu MD. Absorption of sulphur dioxide with sodium citrate buffer solution in a rotating packed bed. *Chinese J. Chem. Eng.* 2011;19:687-692.
17. Pan WH, Shi YX, Liu JP. The design and development of a mass balance calculation software for sodium-calcium dual-alkali scrubbing flue gas desulfurization. *Appl. Mech. Mater.* 2012;155:27-31.
18. Wang XS, Huang YB, Lin ZJ, Cao R. Phosphotungstic acid encapsulated in the mesocages of amine-functionalized metal-organic frameworks for catalytic oxidative desulfurization. *Dalton T.* 2014;43:11950-11958.
19. Xie WL, Wan F. Immobilization of polyoxometalate-based sulfonated ionic liquids on UiO-66-2COOH metal-organic frameworks for biodiesel production via one-pot transesterification-esterification of acidic vegetable oils. *Chem. Eng. J.* 2019;365: 40-50.
20. Yamamoto Y, Yamamoto H, Takada D, Kuroki T, Fujishima H, Okubo M. Simultaneous removal of $NO_X$ and $SO_X$ from flue gas of a glass melting furnace using a combined ozone injection and semi-dry chemical process. *Ozone-Sci. Eng.* 2016;38:211-218.
21. Tomas-Alonso F. A new perspective about recovering $SO_2$ off gas in coal power plants: Energy saving. Part III. Selection of the best methods. *Energ. Source.* 2005;27:1051-1060.
22. Sipos L. Inhibition of sulfite oxidation by phenols: Screening antioxidant behavior with a clark oxygen sensor. *J. Chem. Educ.* 1998;75:1603-1605.
23. Cui S, Wang LD, Hao SQ, Du LX. Oxidation rate of sodium sulfite in presence of inhibitors. *Energ. Procedia* 2012;16: 2060-2066.
24. Wang LD, Ma YL, Hao JM, Zhao Y. Mechanism and kinetics of sulfite oxidation in the presence of ethanol. *Ind. Eng. Chem. Res.* 2009;48:4307-4311.
25. Siddiqi MA, Petersen J, Lucas K. A Study of the effect of nitrogen dioxide on the absorption of sulfur dioxide in wet flue gas cleaning processes. *Ind. Eng. Chem. Res.* 2001;40:2116-2127.
26. Sima A, Fredrik N, Klas A, Filip J. Modeling the nitrogen and sulfur chemistry in pressurized flue gas systems. *Ind. Eng. Chem. Res.* 2015; 54:1216-1227.
27. Chang JCS, Brna TG. Pilot testing of sodium thiosulfate. *Environ. Prog.* 1986;5:225-233.